



**HAL**  
open science

## PDMS membranes modified by polyelectrolyte multilayer deposition to improve OSN separation of diluted solutes in toluene

Mahbub Morshed, Alexandre Zimmer, Laurent Broch, Halima Alem, Denis Roizard

### ► To cite this version:

Mahbub Morshed, Alexandre Zimmer, Laurent Broch, Halima Alem, Denis Roizard. PDMS membranes modified by polyelectrolyte multilayer deposition to improve OSN separation of diluted solutes in toluene. *Separation and Purification Technology*, 2019, 237, pp.116331. 10.1016/j.seppur.2019.116331 . hal-02391641

**HAL Id: hal-02391641**

**<https://hal.science/hal-02391641v1>**

Submitted on 3 Dec 2019

**HAL** is a multi-disciplinary open access archive for the deposit and dissemination of scientific research documents, whether they are published or not. The documents may come from teaching and research institutions in France or abroad, or from public or private research centers.

L'archive ouverte pluridisciplinaire **HAL**, est destinée au dépôt et à la diffusion de documents scientifiques de niveau recherche, publiés ou non, émanant des établissements d'enseignement et de recherche français ou étrangers, des laboratoires publics ou privés.



# Separation and Purification Technology xxx (xxxx) xxx-xxx deposition to improve OSN separation of diluted solutes in toluene

Mahbub Morshed, Alexandre Zimmer, Laurent Broch, Halima Alem, Denis  
Roizard

## ► To cite this version:

Mahbub Morshed, Alexandre Zimmer, Laurent Broch, Halima Alem, Denis Roizard. Separation and Purification Technology xxx (xxxx) xxx-xxx deposition to improve OSN separation of diluted solutes in toluene. Separation and Purification Technology, Elsevier, In press, 10.1016/j.seppur.2019.116331 . hal-02391641

**HAL Id: hal-02391641**

**<https://hal.archives-ouvertes.fr/hal-02391641>**

Submitted on 3 Dec 2019

**HAL** is a multi-disciplinary open access archive for the deposit and dissemination of scientific research documents, whether they are published or not. The documents may come from teaching and research institutions in France or abroad, or from public or private research centers.

L'archive ouverte pluridisciplinaire **HAL**, est destinée au dépôt et à la diffusion de documents scientifiques de niveau recherche, publiés ou non, émanant des établissements d'enseignement et de recherche français ou étrangers, des laboratoires publics ou privés.

# PDMS membranes modified by polyelectrolyte multilayer deposition to improve OSN separation of diluted solutes in toluene

Mahbub Morshed<sup>a</sup>, Alexandre Zimmer<sup>b,c</sup>, Laurent Broch<sup>d</sup>, Halima Alem<sup>b</sup>, Denis Roizard<sup>a,\*</sup>

<sup>a</sup> Laboratoire Réactions et Génie des Procédés (LRGP), UMR 7274 CNRS-UL, Université de Lorraine, 1, rue Grandville, 54000 Nancy, France

<sup>b</sup> Institut Jean Lamour (IJL), UMR CNRS 7198, Université de Lorraine, 2 allée André Guinier, Campus Artem, 54011 Nancy, France

<sup>c</sup> Laboratoire Interdisciplinaire Carnot de Bourgogne (ICB), UMR 6303 CNRS, Université de Bourgogne, 9 Avenue Alain Savary, BP47870, 21078 Dijon Cedex, France

<sup>d</sup> LCP-A2MC, Institut Jean Barriol, Université de Lorraine, 1 Boulevard Arago, BP 95823, 57078 METZ Cedex 3, France

## ARTICLE INFO

### Keywords

Polyelectrolytes  
Nanolayer  
Organic solvent nanofiltration (OSN)  
PDMS  
R-BINAP  
C44

## ABSTRACT

New functionalized poly(dimethylsiloxane) (PDMS) membranes were prepared by the surface modification of the commercially available PERVAP4060 membrane (Sulzer™) through cold plasma activation followed by the layer-by-layer assembly method. Four different pairs of polyelectrolytes, i.e., poly(allylamine hydrochloride) (PAH)/poly(acrylic acid) (PAA), PAH/poly(sodium 4-styrene sulfonate) (PSS), poly(diallyldimethylammonium chloride) (PDDA)/PAA, and PDDA/PSS, were used to coat the PDMS layer by the controlled deposition of successive nanolayers (20–50 nm). PERVAP4060 was systematically modified by the deposition of 10 bilayers of polyelectrolyte pairs. These membranes were characterized by contact angle measurements, scanning electron microscopy (SEM), ellipsometry, and atomic force microscopy (AFM). The nanofiltration membrane performance for the rejection of four diluted solutes—two soluble catalysts 2,2'-bis(diphenylphosphino)-1,1'-binaphthyl (R-BINAP) and tetraoctylammonium bromide (ToABr) and two linear aliphatic molecules *n*-Tetratetracontane (C<sub>44</sub>H<sub>90</sub> or C44) and *n*-Hexadecane (C<sub>16</sub>H<sub>34</sub> or C16)—was studied in the toluene feed solution at up to 40 bar pressure. It was shown that the organic solvent nanofiltration (OSN) mass transfer properties differ clearly depended on the layer-by-layer chemical structure and the characteristics of the solutes. Thus, the intrinsic permeance of toluene in the PEL multilayers were calculated by applying resistance-in-series model. Despite the highly diluted concentrations of the solutes, i.e., < 1 wt% for R-BINAP and ToABr, and the high solvent permeate flux, the ToABr, R-BINAP, and C44 solutes were markedly rejected by all the membranes. ToABr had the highest rejection coefficient, up to 97%. As a trend, higher the polarity of the bilayer assembly, lower was the mass transfer of the solvent compared to that of the pristine membrane. The results indicated that a solution-diffusion mechanism is likely to apply. The best rejection of R-BINAP (up to 88%) was obtained when the membrane was coated with 10 bilayers of PAH/PSS. Thus, these prepared polyelectrolyte (PEL)-modified membranes have potential applications in homogeneous catalysis industry, for example in olefin metathesis for expanding the lifetime of soluble catalysts by separating them at mild OSN condition while ensuring the permeation of products.

## 1. Introduction

Organic solvent nanofiltration (OSN) is a promising membrane technology for the purification of liquid mixtures. In this process, a pressure gradient is applied to the liquid feed to enable the solute/solvent separation by selective permeation through a membrane. The biggest molecule is expected to be rejected from the permeate flux. The most successful application of this process was carried out by Exxon Mobil in the 2000s, when they recycled the solvent used for the purification of lube oils. The main challenge nowadays is the development of membranes that would demonstrate both high permeance and high rejection

performance in organic media for application in diverse industries such as fine chemistry, soluble catalyst recycling, oil and solvent purification, and solvent exchange [1]. In that sense, approximately two decades ago, Mulder et al. [2] classified nanofiltration membranes based on the pressure required to achieve the target separation, i.e., between 5 and 20 bar. Currently, the major challenge is to maintain the time operating stability of the membrane performance at up to 40 bar under different feed conditions as well as other harsh conditions. Therefore, polymeric membranes with high resistance towards solvents, i.e., enhanced stability toward organic solvents and compaction, were developed [2–5]. The most well-known membranes are polyimides, poly(ether-ether-ketone), poly(dimethylsiloxane) (PDMS), and poly-

\* Corresponding author.

E-mail address: denis.roizard@univ-lorraine.fr (D. Roizard)

benzimidazoles [5,6]. The number of membranes is limited owing to the required chemical, mechanical, and thermal membrane stabilities, which are crucial for the targeted application. However, the biggest challenge up to now is that OSN membrane performance is not predictable from one organic solvent to another.

It has been shown that a good alternative to avoid new material synthesis and development is to alter the membrane surface to tailor the interactions between the membrane and the solvent and/or solute [7–9]. The past decades have, therefore, witnessed the growth of surface functionalization processes such as plasma treatment [10], UV light treatment [11], and covalent and supramolecular grafting of macromolecules [7,12,13]. The layer-by-layer assembly (LBL) of polyelectrolytes (PELs) is one of the most promising processes owing to its versatility and the fact that it can be conducted under environment-friendly conditions, both for aqueous and organic nanofiltration. Moreover, the LBL method is inexpensive and enables the building of thin films with a nanometer scale control [12,14,15].

Further, recent works have shown that the layer-by-layer assembly of polyelectrolytes can create stable nanofiltration membranes that are well-resistant to organic solvents with very high flux and selectivity [7–9,16,17]. The LBL process, developed by Decher [14,18], consists of the alternating deposition of polyelectrolytes with opposite charges in water media. The complex presents unique properties owing to the strong internal Coulomb interactions and the possibility of tuning the final deposited film just by modifying the chemical nature of the polyelectrolyte or more simply the pH, the ionic strength, or layer number. Moreover, the final complex is insoluble in a wide range of organic solvents.

To the best of our knowledge, PDMS has been rarely used as support for PEL deposition and has never been used in OSN as a composite-PEL membrane. As PDMS is highly hydrophobic and PEL highly hydrophilic, it is rather counterintuitive to associate them in a composite film. Nevertheless, the PDMS surface is slightly negative and favors the initial adsorption of poly(diallyldimethylammonium chloride) (PDDA). Benavidez [19] reported the preparation and use of PDDA/poly(sodium 4-styrene sulfonate) (PSS)-modified PDMS films for application in capillary electrophoresis. Kumlangdudsana also reported the use of PDDA/PSS on a PDMS substrate to improve organic resistance in microfluidic applications [20].

To ensure the stability of the LBLs on PDMS and resistance to the mechanical shear stress under the cross-flow OSN operating conditions, a plasma-activating procedure has been used. Indeed it has been shown in previous work [7] that very stable polyelectrolyte layers could be obtained even on PDMS by combining cold plasma activation followed by the layer-by-layer assembly of PDDA and PSS. In this work, we transposed this plasma-activated process to the layer-by-layer assembly of three other pairs of polyelectrolytes, i.e., poly(allylamine hydrochloride) (PAH)/poly(acrylic acid) (PAA), PAH/PSS, and PDDA/PAA, on a PDMS-based commercial membrane, PERVAP4060 (Sulzer™).

The objective of this work was to study the rejection by OSN of four solutes—two soluble catalysts, *R*-BINAP and ToABr, and two linear aliphatic molecules, C44 and C16, diluted in toluene—and to compare the outcome with the rejection results of pristine PERVAP4060 [21]. It was envisioned that the deposition of bilayers at the nanometer scale on PERVAP4060 could help to improve the rejection of solutes, first, by decreasing the swelling of the PDMS layer and, second, by increasing and tuning the charge density of the top layer in contact with the feed, whereas the total flux would remain rather high in relation to the very small thickness of the polyelectrolyte layer.

## 2. Materials and methods

### 2.1. Chemicals

*R*-BINAP (white powder; purity >94%), ToABr (white powder; purity 98%), *n*-hexadecane (purity >99%), and tetratetracontane (C44, purity 99%) were purchased from Sigma-Aldrich and used as received. Toluene (purity 99.8%) was also obtained from Sigma-Aldrich.

Commercial PERVAP4060 is a composite membrane having a dense top layer made of PDMS (thickness: 1–2 μm) obtained from DeltaMem AG (www.deltamem.ch). The modified membranes were obtained from the deposition of multilayered films from a couple each of strong and weak polyelectrolytes purchased from Sigma-Aldrich, namely, PDDA (molecular weight  $M_w = 100,000\text{--}200,000\text{ g}\cdot\text{mol}^{-1}$ ) and PAH ( $M_w = 150,000\text{ g}\cdot\text{mol}^{-1}$ ) as cationic polyelectrolytes and PSS ( $M_w = 70,000\text{ g}\cdot\text{mol}^{-1}$ ) and PAA ( $M_w = 1,250,000\text{ g}\cdot\text{mol}^{-1}$ ) as anionic polyelectrolytes. They were used as received. Deionized water (MilliQ® water, 18 MΩ) was used for all the experiments, polyelectrolyte solutions, and cleaning steps.

### 2.2. Plasma treatment

A microwave post-discharge reactor consisting of a cylindrical glass chamber (3 cm in diameter), pumped through a primary pump was used; the plasma was generated by a 2.45 GHz microwave generator. The PDMS was placed into the plasma glass tube at 30 cm from the gas inlet at a residual vacuum of  $10^{-2}$  mbar. The plasma atmosphere consists of an argon and oxygen gas mixture with a flow rate of 400 standard cubic centimeters per minute (sccm) and 40 sccm, respectively. It is critical to carefully control the exposure time to avoid any surface ablation. Under these conditions, a short period of plasma exposure, 30 s, was sufficient. Then the system was vented up to atmospheric pressure and the sample was immediately removed from the reactor and used for the LBL deposition steps. The details of the plasma surface modification have been reported previously by Bassil et al. [7].

### 2.3. LBL membrane modification technique

A concentration of  $10^{-2}\text{ mol}\cdot\text{L}^{-1}$  was used for all the polyelectrolyte aqueous solutions (PDDA, PAH, PAA, and PSS). The pH of the PAA and PAH solutions and the rinsing bath were adjusted at 6.5 to ensure maximum ionization of these weak polyelectrolytes as shown by Choi et al. [22].

The layer-by-layer deposition was conducted in static mode by using the ND-3D, which is a three-axis controlled system developed by Nadatech Innovations. Bilayers were created only on the top surface of the PDMS. First, the PDMS membrane positioned by clamps was immersed in the polycation solutions for 10 min, followed by three rinsing steps (15 dips of 1 s each, 3 dips of 5 s each, and 1 dip of 15 s). Finally, the membrane was immersed in the polyanion solutions for 10 min, followed by the same rinsing steps. Thereby, one bilayer or one cycle of self-assembly membrane was deposited. Additional bilayers were deposited similarly until the target number of bilayers was achieved.

### 2.4. Membrane characterizations

#### 2.4.1. Scanning electron microscopy for original PDMS, plasma-treated PDMS, and polyelectrolyte-modified PDMS

The surfaces of the plasma-modified PDMS and the polyelectrolyte-modified PDMS, prepared by LBL self-assembly, were investigated by scanning electron microscopy (SEM; JEOL 6490LV) at a high vacuum mode (pressure =  $10^{-4}$  Pa).

#### 2.4.2. Atomic force microscopy

The morphologies of the PDMS and the polyelectrolyte-modified PDMS were characterized by atomic force microscopy (AFM) in intermittent-contact mode (tapping mode) on an Asylum Research MFP-3D Infinity™ equipped with a 100- $\mu\text{m}$  close-loop scanner. AFM probes (from Asylum Research) were used in this characterization. The cantilevers had a resonance frequency of approximately 270 kHz and spring constant value of approximately  $26 \text{ N}\cdot\text{m}^{-1}$ . Images were acquired in the air at ambient temperature with a drive amplitude of 15 mV and an attenuation set-point of 0.7–0.8. At least five different zones were scanned on each sample and images at different magnifications were acquired (we have only shown the  $1 \times 1 \mu\text{m}^2$  images). The images were treated and analyzed using procedures developed under Igor Pro (Wavemetrics) by Asylum software.

#### 2.5. Ellipsometry

Silicon wafers, boron-doped, type-*p*, Si (1 0 0), were used for thickness measurements by ellipsometry. First, the wafers were cleaned by Piranha solution (30% hydrogen peroxide and sulfuric acid in 1/1 v/v) for 20 min and followed by three MilliQ® rinsing steps. *Ex situ* variable angle spectroscopic ellipsometry measurements were carried out using a phase-modulated spectroscopic ellipsometer (UVISEL, Horiba Jobin Yvon). Multiple sample analysis [23] was performed using the commercially available DeltaPsi 2 software. Typical ( $I_s$ ,  $I_c$ ) measurements were done for incidence angles between  $60^\circ$  and  $70^\circ$  in steps of  $5^\circ$ , and the wavelength range of the spectrum was 260–860 nm in steps of 5 nm.

#### 2.6. Water contact angle measurements

The water contact angles (WCAs) were measured by using a Digidrop contact angle meter. The setup consists of a white light source, a sample holder (a flat surface), and a camera in the same horizontal plane. The syringe-type milliQ drop dispenser was mounted perpendicular to the flat surface. The setup allows one to see a  $10 \times$  magnification of the dispensed droplet of water and, finally, the WinDrop software was used for data acquisition with an accuracy of  $\pm 0.7^\circ$ .

Both the pristine and polyelectrolyte-modified PDMS samples were dried with a hand drier prior to placing them on the horizontal flat surface of the contact angle meter. Approximately, 1–2  $\mu\text{L}$  of milliQ water was dispensed on the surface and the contact angle was measured within 5–7 s. At least five data points were taken from the different positions of the same sample and a minimum of five different samples were tested for reproducibility.

The optimization of plasma exposure time and hydrophilicity changes of PDMS before and after modification were recorded.

#### 2.7. Cross-flow nanofiltration experiments

The OSN setup consists of a rectangular cross-flow cell (GE Osmonics) that is used in the tangential cross-flow mode, in which the pressure, feed flow rate, and temperature of feed can be well-controlled. This setup has already been reported in the previous papers of Ben Soltane et al. [24,25]. The applied pressure was regulated by using an IP 65 solenoid valve connected with the digital pressure transmitter system and controlled by the Flow DDE Bronchort software [21]. The system allows a precise pressure control over the 1–40 bar range with fluctuation of 0.5–1% to the set value. The temperature was controlled by a Thermo Haake K50 with a precision of  $\pm 1^\circ\text{C}$  and the cross-

flow was set to 7–10 kg/h, measured by a Cori flow (digital mass flow) meter.

Prior to the OSN experiments, the membrane coupons were immersed overnight in the solvent at room temperature as a pre-conditioning step. The membrane coupons used measured  $8 \text{ cm} \times 12 \text{ cm}$  (including the area of the O-ring), corresponding to the effective useful membrane area of  $2.8 \times 10^{-3} \text{ m}^2$ . The coupon was mounted wet into the OSN cell for pressure conditioning. Then the feed flow was maintained at 10 kg/h at  $30^\circ\text{C}$ . Next, a transmembrane pressure (TMP) of 10 bar was applied with a step increase of 2–3 bar using the flow DDE software interface. At each step, the set point with respect to the actual value in the OSN was monitored for the stability of TMP in the upstream. As soon as the pressure of 10 bar was achieved, the unit was monitored for 10–15 min, ensuring stable pressure, cross-flow, and temperature. The same procedure was repeated at 20 bar, 30 bar, and 40 bar. The overall pressure-conditioning cycle was applied systematically to all the used coupons. After conditioning at 40 bar, the TMP was gradually decreased to atmospheric pressure. The aim of this step was to check possible hysteresis effects owing to the increase in pressure. Organic solvent nanofiltration experiments were then performed in a cross-flow rig and in a continuous mode. The permeate was continuously recycled to ensure the steady-state concentration of the feed, i.e., initially 0.05 wt% of the solute.

##### 2.7.1. Permeate measurements

At least 3–5 g of permeate were collected and weighed for each data point and the corresponding time was recorded. At each applied pressure, at least three permeate samples were collected at intervals of a minimum of 20 min. The sample size, number of repetitions, and interval between each sample collection confirm the accuracy of the measurement and stability of the system. Most experiments were repeated more than two or three times using new membrane coupons from different batches.

The flux ( $J$ ) and rejection ( $R$ ) were calculated according to the formulas given below:

$$J = V/(A.t) \quad (1)$$

where  $J$  is the flux ( $\text{Lm}^{-2}\text{h}^{-1}$ ),  $V$  is the volume of the collected permeate (L),  $A$  is the active surface area ( $\text{m}^2$ ), and  $t$  is the time (h);

$$R(\%) = (1 - C_p/C_f) \cdot 100 \quad (2)$$

where  $C_p$  is the concentration of the solute in permeate and  $C_f$  is the concentration of the feed.

##### 2.7.2. Gas chromatography as analytical method for concentration determination

The quantitative analysis of the solutes was carried out using gas chromatography. The operational conditions of the analysis method were as follows:

- Column: HP-5 phenyl methyl siloxane ( $15 \text{ m} \times 320 \mu\text{m} \times 0.25 \mu\text{m}$ ). Flame Ionization Detector (FID):  $380^\circ\text{C}$ , Helium (He): 1 bar.
- Oven program temperature of  $325^\circ\text{C}$  for *R*-BINAP using tetratetracontane ( $\text{C}_{40}\text{H}_{82}$ ) as an external standard. The calibration and one typical chromatogram are illustrated in [21].
- Oven program temperature of  $200^\circ\text{C}$  for ToABr and *n*-hexadecane using *n*-tetracosane ( $\text{C}_{24}\text{H}_{50}$ ) as an external standard.

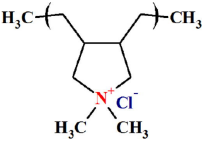
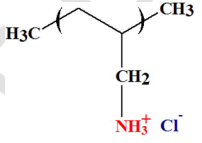
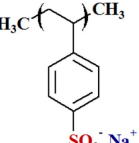
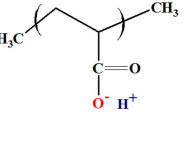
As the solutes had low concentrations (0.1–0.05 wt%), the calibration curve and measurements were carried out using suitable external standards and the constant volume addition method. Each sample test was triplicated and the different experimental results were compared for the determination of solute rejection.

### 3. Results and discussion

#### 3.1. Choice and characteristics of PELs

Hundreds of PELs are commercially available. Up to now, there has been no guideline to choose the PEL according to the type of separation being studied. In this work, only four PELs have been used, two cationic and two anionic, to give rise to the LBLs of various charge density. Indeed, in organic media, charge density acts as a physical cross-linker and it has been expected that the average charge concentration could influence the mass transfer by tuning the local network mobility and hence the diffusion coefficient of the permeant. The data collected to characterize the PELs are presented in Table 1. Using either the Fedor group contribution method or the HsPiP software, it has not been possible to obtain coherent values of the Hansen solubility parameters for the PEL because the ionic part of the PEL could not be considered. Instead, the average charge density of the structure was calculated for each PEL. It was found that the charge density varied within a wide range, from 1 to 3, referring to the molar weight of the PEL repeating unit. PSS has the lowest charge density whereas PAA and PAH are endowed with higher values, up to three times for PAH compared to PSS. Giving rise to physical cross-linking via ionic interactions, these charge densities might explain partly the high glass transition temperatures reported in the literature for the PELs (Table 1) [26–31].

**Table 1**  
Main characteristics of PDMS and the PEL employed.

Polymer	Monomer unit	MW unit (g. mol <sup>-1</sup> )	Mn <sup>b</sup> (g)	pKa <sup>c</sup>	T <sub>g</sub> <sup>d</sup> (°C)
PDMS	(Me <sub>2</sub> OSi) <sub>n</sub>	74	NA	NA	-123
PDDA	(C <sub>8</sub> H <sub>16</sub> N) <sub>n</sub>	125.5	≈200 000	7	67
PAH	C <sub>3</sub> H <sub>6</sub> N	57.5	150 000	9.5	>190
PSS	[C <sub>8</sub> H <sub>7</sub> SO <sub>3</sub> <sup>-</sup> ] <sub>n</sub>	183	70 000	1	180
PAA	(C <sub>3</sub> H <sub>3</sub> O <sub>2</sub> ) <sub>n</sub>	71	1 250 000	4.25	80–128
PELstructure					
Charge density <sup>a</sup> by weight (×10 <sup>-3</sup> )	PDDA, cationic strong 8.01	PAH, cationic weak 17.49	PSS, anionic strong 5.55	PAA, anionic weak 14.17	
Reduced value	1.45	3.18	1	2.57	

<sup>a</sup> Calculated according to the formula, Charge density = 1/Mw<sub>monomer</sub>.

<sup>b</sup> Number average molecular weight (M<sub>n</sub>).

<sup>c</sup> Acid dissociation constant (K<sub>a</sub>) of a solution.

<sup>d</sup> Glass transition temperature (T<sub>g</sub>).

**Table 2**  
Main characteristics of the composite LBL formed on PERVAP4060 modified with 10 bilayers. The root-mean-square value as calculated from AFM images (10 × 10 μm<sup>2</sup>).

Surface modification	Pristine PDMS	Plasma activation	PDDA/PSS	PDDA/PAA	PAH/PSS	PAH/PAA
α (°) (±2) <sup>a</sup>	103	19	77	55	79	47
rms (nm) <sup>b</sup>	1.6	1.6	3.4	25.2	3.9	NA
T <sub>g</sub> (°C) <sup>c</sup>	-123		90	NA	167	45
Thickness (nm ± 0.5) <sup>d</sup>	1500		25	51	25	62

<sup>a</sup> Water contact angle.

<sup>b</sup> Rugosity measured by AFM.

<sup>c</sup> [26,29,32–34].

<sup>d</sup> Measured by ellipsometry, except PDMS layer [25].

#### 3.2. PDMS surface modification

As previously shown by Bassil et al. [7], to ensure good stability and homogeneity of the polyelectrolyte depositions, the PDMS surface was activated by cold plasma post-discharge of Ar/O<sub>2</sub> to generate negative charges at the polymer surface to make it able to anchor the first layer of the cationic polyelectrolyte. Subsequently, the four different couples of polyelectrolytes were assembled layer by layer, up to 10 bilayers, to guarantee good coverage, using an automatic coater to ensure good reproducibility:

- PDDA/PSS—one LBL built with strong polyelectrolytes;
- PAH/PSS and PDDA/PAA—two LBLs associating the strong and weak polyelectrolytes; during the procedure, the pH was adjusted to a value of 6.5 to ensure strong dissociation of PAH and PAA; and
- PAH/PAA—one LBL associating two weak PELs. The pH of the coating solution was also adjusted to 6.5 for PAA to enhance the ionization of both PELs.

These composite LBL-modified PDMS membranes were characterized by several techniques to determine the properties of the LBL surface. The results are reported in Table 2.

After plasma exposure, the PDMS membrane exhibits a very low water contact angle (WCA), 19° (±2), compared to that of the pristine membrane, 100°, in relation with the negative charge created on the PDMS surface. It was shown that when the plasma-treated membrane is maintained under room temperature, the WCA slowly increases

(see Supplementary Fig. SM1). To avoid the drawbacks of the PDMS hydrophobicity recovery [7], the PEL depositions were conducted soon after the plasma activation, within 45 min. The WCAs measured after the LBL deposition are shown in Table 2. In all cases, the WCA was markedly increased while, however, remaining lower than the virgin WCA of the pristine membrane, as expected. It should be noted that the contact angles of the PEL-modified PERVAP4060 were stable with respect to time. Repeated measurements after OSN experiments also confirmed the stability. The LBLs prepared gave rise to two types of contact angles, i.e.,  $\alpha \approx 78^\circ$  or  $\alpha < 56^\circ$ . It may be noted that the two higher WCAs characterize the LBLs whose last layer is PSS, whereas the two lower ones characterize the LBLs having PAA as a final deposited layer. This difference is well in agreement with the charge density that characterized each PEL—the highest one (PAA) corresponds to the lowest WCA.

The LBLs built with PAA also have another peculiarity—they are thicker (50/60 nm) than the two others LBLs (approximately 25 nm). As a rule, any phenomenon that has the potential to slow down the chain relaxation process and limit chain spreading when adsorbing the PEL can favor the formation of thicker layers [35]. The high molecular weight of PAA ( $M_w = 1,250,000$  Da) used in this work might gener-

ate entanglements and, thus, be the reason for the higher thickness of the LBL containing PAA.

The homogeneity of surface was studied by combining SEM for the large-scale investigation (see Supplementary Fig. SM2) and AFM (in the tapping mode) for the nanometric scale.

As shown in Fig. 1 with some AFM examples, the modified surfaces are quite different from the pristine PDMS surface; tuning the chemical structure of the PDMS layer also translates into a different root-mean-square (rms) roughness, which increases by up to 3.3 nm for the PDDA/PSS, to reach 25.2 nm for the PDDA/PAA (Table 1). The PDDA/PAA assembly led to thicker and rougher surfaces compared to the PDDA/PSS, which is consistent with the highly coiled chains conforming to the behavior of well-known weak polyelectrolytes [12,36,37].

The local charge density of each bilayer unit has also been calculated as in the case of the PEL unit, using the molar mass PEL pairs forming the LBL. As expected from the PEL properties, the four deposited LBLs cover a large range of charge density, going from 1 to 2.4 times in the increasing order PDA/PSS < PAH/PSS < PDDA/PAA < PAH/PAA (see Table 3).

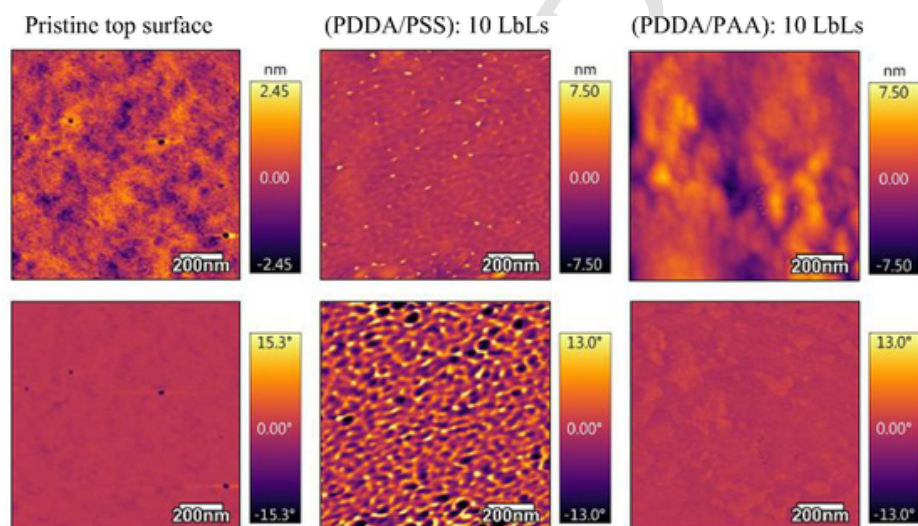


Fig. 1. Topographic (top) and phase (bottom) AC-mode images of PERVAP4060 and related modified LBL multilayer (10 cycles).

Table 3  
Calculated parameters of the LBLs to address interactions with the solute.

LBL structural unit				
Charge density <sup>a</sup>	PDDA/PSS	PDDA/PAA	PAH/PSS	PAH/PAA
By weight ( $\times 10^{-3}$ )	3.24	5.09	4.15	7.7
Reduced value	1	1.6	1.3	2.4
Toluene flux (kg/(h·m <sup>2</sup> ))	42	7	35	16
Predicted flux (20 bar, 30 °C)	42	23	33	17

<sup>a</sup> Charge density calculated as  $1/M_{w,monomer}$



#### 4. Investigation of the OSN properties of the modified PERVAP4060

##### 4.1. Effect of plasma treatment on OSN flux

In the first step, the potential effect of the plasma treatment on the OSN mass transfer was investigated only with toluene as the feed. The results shown in Fig. 2 indicate that the plasma procedure used does not modify the permeability of the active layer. It means that no significant cross-linking of the network occurred, neither was there any ablation. Indeed, these two drawbacks can be observed when inadequate plasma parameters are used.

##### 4.2. Investigation of the number of LBLs on OSN flux

In the second step, the influence of the number of deposited LBLs on the toluene flux was investigated. Indeed, the PELs used to deposit the LBLs are all characterized in the dry state by a high glassy transition temperature up to 190 °C for PAA (Table 1). The reported  $T_g$  data of the corresponding LBLs are also characterized by glassy structures (Table 2) [32,33]. Hence, it was expected that the modified LBL membranes would have much lower permeances than the pristine PERVAP4060, whose selective layer, PDMS, is known to have a rubbery structure characterized by a very low  $T_g$  (-123 °C).

As shown in Fig. 3, the flux with 5 LBLs of PDDA/PSS was almost unchanged, whereas the flux with 10 LBLs was decreased by approximately 20%. Therefore, in the further LBL deposition, this number, of 10 bilayers, was maintained as a standard to ensure full PDMS surface coverage.

##### 4.3. Study of effect of LBL composition (10 bilayers) on toluene OSN flux

Prior to the study of the binary and ternary feed mixtures, the toluene mass transport was characterized for the four membranes up to 20 bar. The data presented in Fig. 4 show a linear increase of the flux with the transmembrane pressure (TMP) for each LBL type, leading to very different values of toluene fluxes, which vary in the proportion 1 to 7. On the other hand, no hysteresis effect could be detected with respect to time. This indicates that the modified membranes were well stable with respect to the pressure and the shear stress induced by the tangential feed flow, tested up to 20 L/h.

To explain the flux variation, the LBL composition was considered first. However, no simple relationship could be drawn between the oc-

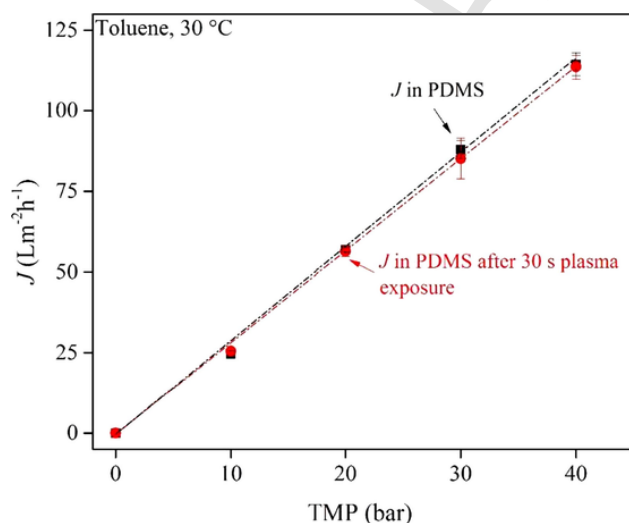


Fig. 2. Evaluation of plasma treatment on toluene OSN flux (30 °C).

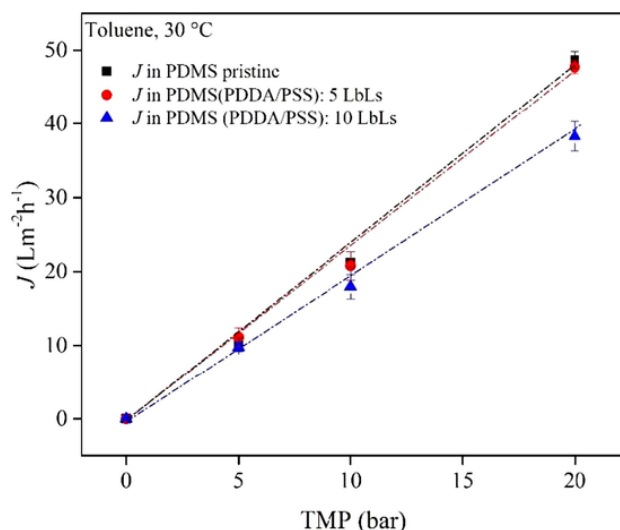


Fig. 3. Effect of number of bilayers (PDDA/PSS) in toluene OSN fluxes (30 °C).

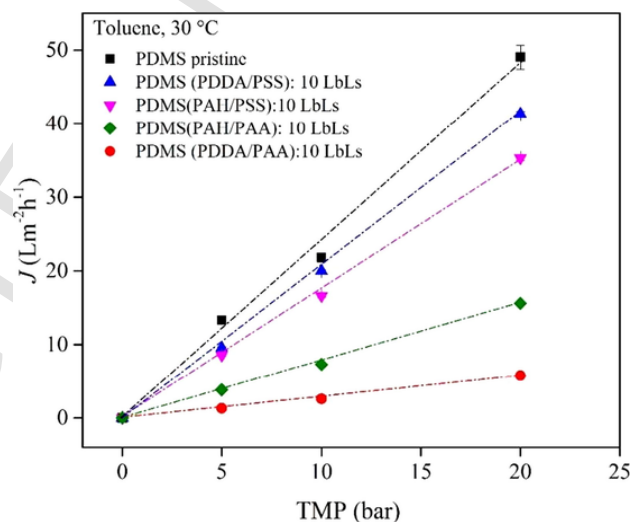


Fig. 4. Effect of PEL modification of PERVAP4060 on toluene flux (30 °C) recorded in tangential mode (20 L/h).

currence of each PEL and the measured fluxes. Indeed, PDDA is, for instance, a part of the modified membrane having the higher flux (PDDA/PSS) and a part also of the modified membrane having the lowest flux.

Therefore, another way to evaluate the intrinsic permeability of each LBL has been researched. For a dense network, it is well-known that two major factors determine the permeability: the affinity properties with the penetrant, the toluene molecules in this study, and the diffusion coefficient of the penetrant, which is controlled by the stiffness of the network. Usually, the affinities can be evaluated using the Hansen solubility parameters (HSP). Unfortunately, with ionic species, HSP cannot be calculated with the Fedor contribution group method (Table 3).

The charge density (CD) of the LBLs was considered in turn and calculated, as done previously, to be equal to  $1/(\Sigma Mw)$ . Indeed, the charge density accounts for the cross-linking degree of the LBL structure and, thus, for the chain mobility that can tune the diffusion coefficient of a penetrant. First, it was found that the higher solvent fluxes correspond to the LBLs having smaller charge density, i.e., PDDA/PSS and PAH/PSS. Second, it was observed that the fluxes of these two LBL membranes could be predicted by dividing the flux obtained for  $CD = 1$  (re-



duced value) by the charge density of each LBL (Table 3). Only the flux of the PDDA/PAA was not predicted.

#### 4.4. Study of solutes rejection by OSN in toluene solutions

Several series of OSN experiments were carried out with binary feed solutions to mimic the industrial context where catalysts are always used under very high dilution. The chemicals used are reported in Table 4. Besides the experiments with *R*-BINAP and ToABr, the rejection of the two linear alkanes, C44 (*n*-tetratetracontane) and C16 (*n*-hexadecane) have also been studied to evaluate the effect of the molecular size and chemical nature of the solute. In all experiments, high dilutions of the solutes were used in the range 0.05–0.1 wt% in toluene. Gas chromatography was used to determine solute concentrations in the feed and in the permeate solutions with the help of calibration curves using external references (see the Materials and Methods section). *R*-BINAP, ToABr, and C44 are bulky molecules having the same range of molecular weight, i.e., 546–622 g/mole, but ToABr is a charged molecule, a quaternary alkyl ammonium bromide. C44, a linear alkane, and ToABr have higher molar volumes ( $V_m$ ) because of their linear alkyl structure. Indeed *R*-BINAP, which has a polyaromatic structure, is a more rigid and more compact molecule, i.e., approximately 30% more.

Referring to the Hansen solubility parameters (HSP), the relative affinities for the pristine PDMS membrane are in the increasing order: ToABr < *R*-BINAP < C44 < C16. The same order also occurs with toluene. Referring to the LBL-modified PDMS membranes, HSP cannot be used to predict affinities, as already explained in the previous paragraph. However, ToABr being a charged molecule, strong interactions with the non-polar siloxane network and with the cationic PEL embedded in the LBL structure can be expected.

At this step, before examining the OSN rejection results in detail, it is worth recalling that for a composite membrane, the fluxes and rejection values are the result of the two distinct, dense, and consecutive layers, and each of them has their own intrinsic properties. According to the model of the resistance-in-series [38], for a given component *i*, the effective mass transfer  $Q_i$  through the composite membrane is given by Eq. (3):

$$Q_i = Pe_i \Delta a_i A \quad (3)$$

where  $Pe_i$  is the permeance ( $Pe_i = P_i/l$ ),  $\Delta a_i$  is the activity gradient, and  $A$  is the membrane area.

Next, the intrinsic permeance in PEM has been calculated (Table 5) applying Eq. (3), using toluene fluxes from Fig. 4 and the thickness from Table 2.

The calculated permeance of toluene through PEM shows a high barrier effect for toluene, especially for PELs having no aromatic ring in their skeleton (See PEL structures in Tables 1 and 3).

In Table 5, one can note that the PEMs having PSS show lower barrier effect than the rest. In the literature, it is reported that 30 nm PSS film can swell up to  $\approx 27\%$  in toluene vapor [40]. It is interesting to note that PSS also is endowed of the lowest charge density among four PELs (Table 1). This result is well in agreement with the work of Miller et al (2005) who reported that the polyelectrolytes having lower charge density exhibits higher swelling [41], suggesting PSS is able to swell the most in toluene among the four used PELs, listed in Table 1. Next, when multilayers are formed, PEMs with PSS give lower charge densities than PEMs with PAA (Table 5), thereby, PEMs with PSS are expected to swell to a higher extent in toluene, giving rise to relative high toluene permeance when compared with PEMs formed with PAA.

Hence the equivalent mass transfer resistance  $R_m$  of the composite membrane can be written as:

$$R_m = 1/K = 1/k_{m1} + 1/k_{m2} \quad (4)$$

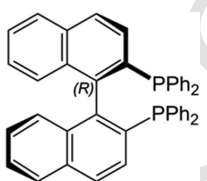
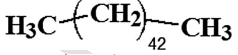
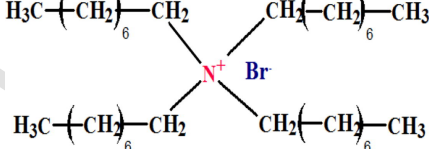

or

$$K = 1/(1/k_{m1} + 1/k_{m2}) \quad (5)$$

where  $K$  is the total mass transfer coefficient of a given component,  $k_{m1}$  and  $k_{m2}$  are the mass transfer coefficients, respectively, through the top layer #1, here the PEL pairs, and through the support layer #2, here the PDMS. The porous support polyacrylonitrile (PAN) layer was not considered here as a resistant layer.

Evidently, the application of this model is valid only under some strict assumptions, postulating steady permeability, no coupling effects between the permeants, and a linear relationship between the permeability and membrane thickness. If these assumptions are likely to

**Table 4**  
Chemicals used to prepare feed solutions and their specifications.

Chemicals	Chemical structure	Mw (gmol <sup>-1</sup> ) $V_m$ (cm <sup>3</sup> mol <sup>-1</sup> )	$\delta$ HSP (MPa <sup>1/2</sup> )
Toluene	Ph-CH <sub>3</sub>	Mw = 92 $V_m$ = 106	18.2
( <i>R</i> )-BINAP		Mw = 622 $V_m$ = 511	21.5
C44		Mw = 619 $V_m$ = 754	16.2
ToABr		Mw = 546 $V_m$ = 761	21.9
C16		Mw = 226 $V_m$ = 294	15.9

**Table 5**  
Intrinsic permeance in PEMs using resistance-in-series model.

PELs, 10 bilayers	Toluene permeance in PEM ( $\text{Lm}^{-2}\text{h}^{-1}\text{bar}^{-1}$ )	Reduction factor <sup>a</sup>	Charge density
PDMS	2.1	–	–
PDDA/PSS	0.45	5	1
PAH/PSS	0.14	15	1.3
PAH/PAA	0.03	70	2.4
PDDA/PAA	0.01	210	1.6

<sup>a</sup> Ratio of permeance in PDMS and PEM.

hold in gas permeation, some deviations from this mechanism can occur at high swelling.

However, Eqs. (4) and (5) shows that the effect of the top layer on the effective mass transfer will strongly depend on the relative values of  $k_{m1}$  and  $k_{m2}$ : the lower mass transfer coefficient will govern the effective permeance and, thus, the rejection of the composite membrane when a mixture of two components is considered.

Overall, this means that six parameters will control the effective permeance and rejection values:

- the permeability of the solvent and of the solute,
- the activity gradient of each permeant, and
- the real thickness for each layer.

In addition to the OSN case, if the mass transfer coefficient of the top layer  $k_{m1}$  is the lowest, as expected with the rigid PEL pairs in toluene, the mass transfer coefficient of the PDMS layer is likely to be reduced owing to the lower swelling degrees of the PDMS network. Clearly, under OSN conditions, the effective permeance of the composite membrane cannot be predicted in a simpler way (see Table 6).

The general trend observed for the rejection of solutes is demonstrated by the pristine PDMS membrane. The solute ToABr, i.e., the charged molecule, has the highest rejection (93%) and the solute C16, being also the smallest molecule, has the lowest rejection (7%). This trend is valid for all the membranes. These results are in agreement both with the HSP and with the size of the molecules (Table 4).

Next, when the rejections of *R*-BINAP and C44 are considered, the values are much closer to each other. For the pristine PDMS, the

**Table 6**  
Results of OSN experiments with binary mixtures using LBL-modified membranes (10 bar, 30 °C, diluted toluene feeds).

Membrane sample	Global flux ( $\text{Lm}^{-2}\text{h}^{-1} \pm 10\%$ )	Rejections of solutes (%) $\pm 2$				Charge density <sup>c</sup>
		<i>R</i> -BINAP <sup>a</sup>	ToABr <sup>a</sup>	C16 <sup>b</sup>	C44 <sup>a</sup>	
PDMS pristine	24	80	70	93	7	NA
PDMS (PDDA/PSS): 10 LBLs	22.9	82	88	92	6.5	1
PDMS (PAH/PSS): 10 LBLs	14	88.5	93	97	7	1.3
PDMS (PAH/PAA): 10 LBLs	7.6	66.3	80	84	10	2.4
PDMS (PDDA/PAA): 10 LBLs	3.8	80.5	82	92	10	1.6

<sup>a</sup> Solute concentration: 0.05 wt%.

<sup>b</sup> Solute concentration: 0.1 wt%.

<sup>c</sup> Reduced charge density.

C44 alkane molecule is less rejected, in agreement with the lower HSP ( $\delta = 16.2$ ) close to the PDMS value ( $\delta = 15.4$ ) [39]. However, with all the LBL-modified membranes, the rejection values of these two solutes are reversed. This clearly seems to be an effect induced by the charged LBL layer, which repels the non-polar C44 alkane molecule. This effect is also observed to some extent with the C16 molecule, with the two LBL membranes having the higher charge density, i.e., PDDA/PAA and PAH/PAA.

With respect to *R*-BINAP rejection, the LBL with 10 layers of (PAH/PSS) exhibits a marked improved rejection, up to 88.5%. The same result is also obtained for the rejection of ToABr and C44. It is, of course, difficult to explain these three results in detail because they are owing to several parameters that are able to affect both the solubility and the diffusion of the solutes, such as the charge density, the LBL's  $T_g$ , and the activity and mobility of the solutes. Nevertheless, as a marked rejection improvement is obtained for the three types of solutes (polyaromatic, charged, and alkane molecules), the reason more likely seems to be a relative decrease of the diffusion of the solute versus toluene diffusion.

Another interesting result is linked to the use of the LBL formed by the PEL pair PAH/PAA, the pair that has the highest charge density (Table 4). Indeed, despite a strong global flux reduction, converse to the results obtained with the previous LBL (PAH/PSS), the rejection values of the two polar solutes, *R*-BINAP and ToABr, are smaller compared to the rejection values obtained with the reference pristine PDMS membrane. Therefore, it seems that this LBL structure is less repulsive for polar solutes than for the others. The reason for this effect is not yet clearly understood but might be linked to the presence of PAA.

#### 4.5. Evaluation of potential aging of (PAH-PSS): 10 LBLs modified PDMS

After conditioning the LBL-modified membranes as usual for 30 min, the long-term stability of the multilayered PAH/PSS film was studied for several days. First, the OSN conditions were applied for several hours at 20 bar and 30 °C under the tangential feed flow mode. The rejection and the fluxes were measured every hour. The related results are shown in Fig. 5, which depicts the relationship of the flux ( $J$ ) and rejection ( $R$ ) with time. Clearly, no deviation was observed and the *R*-BINAP rejection value remained steady at approximately 88%. Thereafter, the pressure was released for two days and reapplied the third day, along with tangential feed flow. Under these operating conditions, the measured flux and rejection values were found to be the same as they were three days before, i.e.,  $38 \text{ L}\cdot\text{m}^{-2}\cdot\text{h}^{-1}$  (TMP = 20 bar) and 88.6%, respectively. This series of experi-

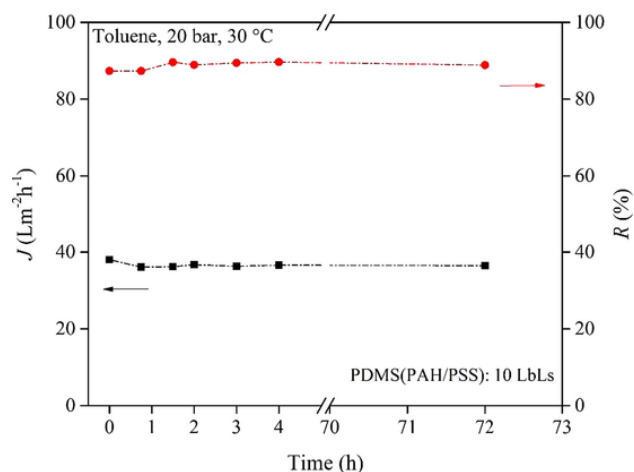


**Fig. 5.** Performance stability with the PAH/PSS-modified PERVAP4060: Rejection of *R*-BINAP in toluene at 20 bar and 30 °C over three days in tangential mode.

ments confirmed the stability of the LBL-modified membrane under OSN conditions and tangential feed flow, and the absence of any fast aging owing to some delamination of the top layer of the LBL.

#### 4.6. Study of OSN performance with a model ternary mixture

Finally, a ternary feed mixture was studied to mimic an industrial case with a simple multicomponent system composed of dilute catalytic ligand (0.05 wt%), the linear saturated hydrocarbon C16 (feed range: 1–10 wt%), and toluene.

The results are shown in Fig. 6. It can be seen that the rejection of C16, close to 9%, is much lower than that for *R*-BINAP and similar to the rejection value previously observed at the feed concentration of 0.1 wt%. This big difference can be easily explained by the higher diffusion coefficient of C16 linked to its smaller size, both in the PEL and PDMS layers.

With the increase in the C16 concentration from 1 wt% to 10 wt%, a small decrease in the *R*-BINAP rejection value was also observed. However, a much significant effect on C16 rejection can be underlined as well as on the global NF flux, which increased by approximately 40%. Clearly, this flux increase was greater than the simple flux contribution of the linear hydrocarbon. This indicates that the permeability coefficients are likely to increase in the presence of C16.

Finally, from a process point of view, these OSN results are quite interesting because this membrane technique would allow easy separation of the linear C16 molecule from *R*-BINAP in a toluene feed mixture. This is a promising result for application in metathesis synthesis.

## 5. Conclusion

The layer-by-layer method allowed an easy modification of the commercial PERVAP4060 membrane. Using a cold plasma pretreatment, four new composite membranes, well-stable in OSN, were obtained with top dense nanolayers allowing the solvent mass transfer and solutes' rejection values to be tuned. Based on the investigations carried out with these membranes using neutral or charged solutes, the following points can be underlined:

- In the range 10–40 bar, well-reproducible results were obtained from toluene feeds, i.e., either binary or ternary mixtures of diluted solutes;
- Except for the smallest molecule, i.e., the alkane C16, high rejection values of the solutes (> 80%) were obtained together with high solvent fluxes (7–21 kg/(h.m<sup>2</sup>)) at 10 bar and 30 °C;

- The four polyelectrolytes used led to the formation of LBLs endowed with various charge densities, which seemed to govern solvent permeation and solute rejection;
- Using 10 bilayers of PEL to functionalize the top surface facilitated distinct OSN performance from the pristine PDMS membrane;
- Higher solvent mass transfer was obtained with the composite membranes having smaller charge density, i.e., PDDA/PSS and PAH/PSS;
- Interestingly, *R*-BINAP, ToABr, and C44 were highly rejected even at very low feed concentration (0.05 wt%); clearly, these results indicate that the transport of the solute must be almost independent of the solvent transport;
- The permeance of toluene due to the PEM layers was calculated applying the resistance in series model. It was shown that the PEM can reduce strongly the mass transfer especially for PEL having high charge density;
- Irrespective of the membrane used, the charged solute ToABr was always the more rejected solute;
- The PAH/PSS pair improved the rejection value of *R*-BINAP compared to the pristine PDMS membrane, up to 88%;
- The total mass transfer and rejection values can be explained in terms of a resistance-in-series model;
- Experiments recorded with a ternary mixture indicate a significant effect of the C16 concentration, which tends to increase the global flux and decrease the C16 rejection. This result seems to be very promising in the context of the potential application of OSN to olefin metathesis;
- Finally, no aging effect could be detected over several days: both the flux and the rejection values appeared to be steady.

To conclude, the charge density of the LBLs and, hence, the LBL rigidity in organic media, seems to be a key parameter that controls the molecular diffusion and, thus, the permeation through the top nanolayers.

#### CRediT authorship contribution statement

**Mahbub Morshed:** Investigation, Validation, Visualization. **Alexandre Zimmer:** Investigation. **Laurent Broch:** Formal analysis. **Halima Alem:** Resources. **Denis Roizard:** Conceptualization, Supervision, Project administration, Funding acquisition.

#### Acknowledgments

This work is a part of the collaborative project, ANR-14-CE06-0022, thanks to the financial support of the French National Research Agency and the support of ARKEMA. Professor S. Abbott is also sincerely acknowledged for the discussion on the Hansen solubility parameters calculations of *R*-BINAP and ToABr. Ellipsometric data were acquired at the Ellipsometry core facility of LCP-A2MC, Université de Lorraine – <http://lcp-a2mc.univ-lorraine.fr>

#### Appendix A. Supplementary material

Supplementary data to this article can be found online at <https://doi.org/10.1016/j.seppur.2019.116331>.

#### References

- [1] P. Marchetti, M.F. Jimenez Solomon, G. Szekely, A.G. Livingston, Molecular separation with organic solvent nanofiltration: a critical review, *Chem. Rev.* 114 (2014) 10735–10806, doi:10.1021/cr500006j.
- [2] L.Y. Ng, A.W. Mohammad, C.Y. Ng, A review on nanofiltration membrane fabrication and modification using polyelectrolytes: effective ways to develop membrane selective barriers and rejection capability, *Adv. Colloid Interface Sci.* 197–198 (2013) 85–107, doi:10.1016/j.cis.2013.04.004.
- [3] D.L. Oatley-Radcliffe, M. Walters, T.J. Ainscough, P.M. Williams, A.W. Mohammad, N. Hilal, Nanofiltration membranes and processes: a review of research trends

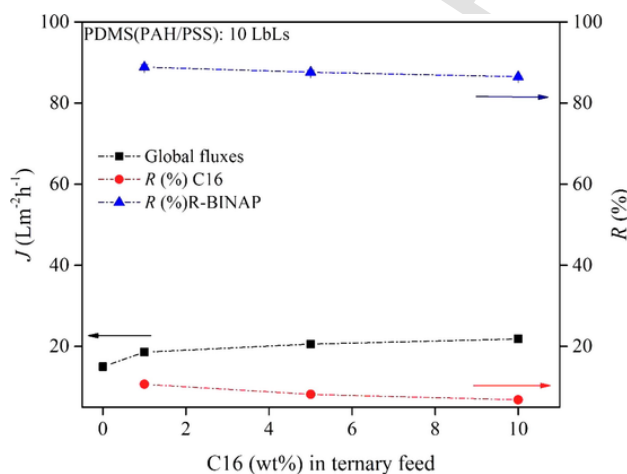


Fig. 6. OSN performance of (PAH-PSS): 10 LbLs modified PERVAP4060 for the separation of a model ternary mixture consisting of C16 (1–10 wt%) and *R*-BINAP (0.05 wt%) in toluene (10 bar, 30 °C).

- over the past decade, *J. Water Process Eng.* 19 (2017) 164–171, doi:10.1016/j.jwpe.2017.07.026.
- [4] A.W. Mohammad, Y.H. Teow, W.L. Ang, Y.T. Chung, D.L. Oatley-Radcliffe, N. Hilal, Nanofiltration membranes review: recent advances and future prospects, *Desalination* 356 (2015) 226–254, doi:10.1016/j.desal.2014.10.043.
- [5] E.J. Kappert, M.J.T. Raaijmakers, K. Tempelman, F.P. Cuperus, W. Ogieglo, N.E. Benes, Swelling of 9 polymers commonly employed for solvent-resistant nanofiltration membranes: a comprehensive dataset, *J. Membr. Sci.* 569 (2019) 177–199, doi:10.1016/j.memsci.2018.09.059.
- [6] J. Liu, Q. Xu, J. Jiang, A molecular simulation protocol for swelling and organic solvent nanofiltration of polymer membranes, *J. Membr. Sci.* 573 (2019) 639–646, doi:10.1016/j.memsci.2018.12.035.
- [7] J. Bassil, H. Alem, G. Henrion, D. Roizard, Tailored adhesion behavior of polyelectrolyte thin films deposited on plasma-treated poly(dimethylsiloxane) for functionalized membranes, *Appl. Surf. Sci.* 369 (2016) 482–491, doi:10.1016/j.apsusc.2016.01.146.
- [8] P. Ahmadiannamini, X. Li, W. Goyens, B. Meesschaert, W. Vanderlinden, S. De Feyter, I.F.J. Vankelecom, Influence of polyanion type and cationic counter ion on the SRNF performance of polyelectrolyte membranes, *J. Membr. Sci.* 403–404 (2012) 216–226, doi:10.1016/j.memsci.2012.02.052.
- [9] X. Li, W. Goyens, P. Ahmadiannamini, W. Vanderlinden, S. De Feyter, I. Vankelecom, Morphology and performance of solvent-resistant nanofiltration membranes based on multilayered polyelectrolytes: study of preparation conditions, *J. Membr. Sci.* 358 (2010) 150–157, doi:10.1016/j.memsci.2010.04.039.
- [10] E.M. Liston, L. Martinu, M.R. Wertheimer, Plasma surface modification of polymers for improved adhesion: a critical review, *J. Adhes. Sci. Technol.* 7 (1993) 1091–1127, doi:10.1163/156856193X00600.
- [11] S. Lazare, V. Granier, Ultraviolet laser photoablation of polymers: a review and recent results, *Laser Chem.* (1989), doi:10.1155/1989/18750.
- [12] H. Alem, F. Blondeau, K. Glinel, S. Demoustier-Champagne, A.M. Jonas, Layer-by-layer assembly of polyelectrolytes in nanopores, *Macromolecules* 40 (2007) 3366–3372, doi:10.1021/ma0703251.
- [13] H. Alem, A.-S. Duwez, P. Lussis, P. Lipnik, A.M. Jonas, S. Demoustier-Champagne, Microstructure and thermo-responsive behavior of poly(N-isopropylacrylamide) brushes grafted in nanopores of track-etched membranes, *J. Membr. Sci.* 308 (2008) 75–86, doi:10.1016/j.memsci.2007.09.036.
- [14] G. Decher, Fuzzy nanoassemblies: toward layered polymeric multicomposites, *Science* 277 (1997) 1232–1237, doi:10.1126/science.277.5330.1232.
- [15] W. Lenk, J. Meier-Haack, Polyelectrolyte multilayer membranes for pervaporation separation of aqueous-organic mixtures, *Desalination* 148 (2002) 11–16, doi:10.1016/S0011-9164(02)00645-8.
- [16] P. Ahmadiannamini, X. Li, W. Goyens, N. Joseph, B. Meesschaert, I.F.J. Vankelecom, Multilayered polyelectrolyte complex based solvent resistant nanofiltration membranes prepared from weak polyacids, *J. Membr. Sci.* 394–395 (2012) 98–106, doi:10.1016/j.memsci.2011.12.032.
- [17] X. Li, S. De Feyter, D. Chen, S. Aldea, P. Vandezande, F. Du Prez, I.F.J. Vankelecom, Solvent-resistant nanofiltration membranes based on multilayered polyelectrolyte complexes, *Chem. Mater.* 20 (2008) 3876–3883, doi:10.1021/cm703072k.
- [18] J. Ruths, F. Essler, G. Decher, H. Riegler, Polyelectrolytes I: polyanion/polycation multilayers at the air/monolayer/water interface as elements for quantitative polymer adsorption studies and preparation of hetero-superlattices on solid surfaces, *Langmuir* 16 (2000) 8871–8878, doi:10.1021/la000257a.
- [19] T.E. Benavidez, C.D. Garcia, Spectroscopic ellipsometry as a complementary tool to characterize coatings on PDMS for CE applications: CE and CEC, *Electrophoresis* 37 (2016) 2509–2516, doi:10.1002/elps.201600143.
- [20] P. Kumlangdudsana, A. Tuantranont, S.T. Dubas, L. Dubas, Polyelectrolyte multilayers coating for organic solvent resistant microfluidic chips, *Mater. Lett.* 65 (2011) 3629–3632, doi:10.1016/j.matlet.2011.07.038.
- [21] M. Morshed, D. Roizard, H. Alem, H. Simonaire, Investigation of OSN properties of PDMS membrane for the retention of dilute solutes with potential industrial applications, *J. Appl. Polym. Sci.* (2019), doi:10.1002/app.48359.
- [22] J. Choi, M.F. Rubner, Influence of the degree of ionization on weak polyelectrolyte multilayer assembly, *Macromolecules* 38 (2005) 116–124, doi:10.1021/ma048596o.
- [23] K. Järendahl, H. Arwin, Multiple sample analysis of spectroscopic ellipsometry data of semi-transparent films, *Thin Solid Films.* 313–314 (1998) 114–118, doi:10.1016/S0040-6090(97)00781-5.
- [24] H. Ben Soltane, D. Roizard, E. Favre, Effect of pressure on the swelling and fluxes of dense PDMS membranes in nanofiltration: an experimental study, *J. Membr. Sci.* 435 (2013) 110–119, doi:10.1016/j.memsci.2013.01.053.
- [25] H. Ben Soltane, D. Roizard, E. Favre, Study of the rejection of various solutes in OSN by a composite polydimethylsiloxane membrane: investigation of the role of solute affinity, *Sep. Purif. Technol.* 161 (2016) 193–201, doi:10.1016/j.seppur.2016.01.035.
- [26] Á. Imre, M. Schönhoff, C. Cramer, A conductivity study and calorimetric analysis of dried poly(sodium 4-styrene sulfonate)/poly(diallyldimethylammonium chloride) polyelectrolyte complexes, *J. Chem. Phys.* 128 (2008), doi:10.1063/1.2901048 134905.
- [27] A. Akyüz, G. Buyukunsal, A. Paril, Online monitoring of diallyldimethylammonium chloride polymerization, *Polym. Eng. Sci.* 54 (2014) 1350–1356, doi:10.1002/pen.23683.
- [28] S.R. Lewis, S. Datta, M. Guí, E.L. Coker, F.E. Huggins, S. Daunert, L. Bachas, D. Bhattacharyya, Reactive nanostructured membranes for water purification, *Proc. Natl. Acad. Sci.* 108 (2011) 8577–8582, doi:10.1073/pnas.1101144108.
- [29] A. Vidyasagar, C. Sung, K. Losensky, J.L. Lutkenhaus, pH-Dependent thermal transitions in hydrated layer-by-layer assemblies containing weak polyelectrolytes, *Macromolecules* 45 (2012) 9169–9176, doi:10.1021/ma3020454.
- [30] H.C. Zhao, X.T. Wu, W.W. Tian, S.T. Ren, Synthesis and thermal property of poly(allylamine hydrochloride), *Adv. Mater. Res.* 150–151 (2010) 1480–1483, doi:10.4028/www.scientific.net/AMR.150-151.1480.
- [31] W. John, C. Buckley, E. Jacobs, Synthesis and Use of Polydadmac for Water Purification, *Water Institute of Southern Africa (WISA)*, 2002, p. 14.
- [32] K. Köhler, D.G. Shchukin, H. Möhwald, G.B. Sukhorukov, Thermal behavior of polyelectrolyte multilayer microcapsules. 1. The effect of odd and even layer number, *J. Phys. Chem. B* 109 (39) (2005) 18250–18259, doi:10.1021/jp052208i.
- [33] Y. Zhang, F. Li, L.D. Valenzuela, M. Sammalkorpi, J.L. Lutkenhaus, Effect of water on the thermal transition observed in poly(allylamine hydrochloride)-poly(acrylic acid) complexes, *Macromolecules* 49 (2016) 7563–7570, doi:10.1021/acs.macromol.6b00742.
- [34] Y. Zhang, P. Batys, J.T. O'Neal, F. Li, M. Sammalkorpi, J.L. Lutkenhaus, Molecular origin of the glass transition in polyelectrolyte assemblies, *ACS Cent. Sci.* 4 (2018) 638–644, doi:10.1021/acscentsci.8b00137.
- [35] P. Nestler, M. Paßvogel, C.A. Helm, Influence of polymer molecular weight on the parabolic and linear growth regime of PDADMAC/PSS multilayers, *Macromolecules* 46 (2013) 5622–5629, doi:10.1021/ma400333f.
- [36] B. Schoeler, G. Kumaraswamy, F. Caruso, Investigation of the influence of polyelectrolyte charge density on the growth of multilayer thin films prepared by the layer-by-layer technique, *Macromolecules* 35 (2002) 889–897, doi:10.1021/ma011349p.
- [37] M. Schönhoff, Layered polyelectrolyte complexes: physics of formation and molecular properties, *J. Phys. Condens. Matter.* 15 (2003) R1781, doi:10.1088/0953-8984/15/49/R01.
- [38] A.J. Ashworth, Relation between gas permselectivity and permeability in a bilayer composite membrane, *J. Membr. Sci.* 71 (1992) 169–173, doi:10.1016/0376-7388(92)85016-C.
- [39] C.M. Hansen, Hansen Solubility Parameters: A User's Handbook, Second Edition, CRC Press, 2007.
- [40] W.H. Ferrell, D.I. Kushner, M.A. Hickner, Investigation of polymer-solvent interactions in poly(styrene sulfonate) thin films, *J. Polym. Sci. Part B Polym. Phys.* 55 (2017) 1365–1372, doi:10.1002/polb.24383.
- [41] M.D. Miller, M.L. Bruening, Correlation of the swelling and permeability of polyelectrolyte multilayer films, *Chem. Mater.* 17 (2005) 5375–5381, doi:10.1021/cm0512225.